Equilibrium Phase Diagrams of Aqueous Mixtures of Malonic Acid and Sulfate/Ammonium Salts

Dara Salcedo*

Centro de Investigaciones Químicas, Universidad Autónoma del Estado de Morelos, Cuernavaca, Morelos, 62209, México

Received: June 20, 2006; In Final Form: August 29, 2006

Tropospheric aerosols are usually complex mixtures of inorganic and organic components. Although the thermodynamic properties of inorganic aerosols have been widely studied, the effect of organics on such properties is still under discussion. In this study, solubility in water, water activity (a_w) of aqueous solutions, deliquescence relative humidity (DRH), eutonic composition, and eutonic DRH were determined for bulk mixtures of malonic acid (MA) with ammonium sulfate (AS) and ammonium bisulfate (ABS) at 25 °C over the full range of composition (from 0 wt % to the solubility limit of the mixture components). The data were used to construct equilibrium phase diagrams, which show the phase of the mixtures as a function of total composition, dry mixture composition, water content, and ambient relative humidity (RH). This work complements previous reports on the thermodynamic properties of AS/MA mixtures because the range of concentrations investigated is larger than in any other published single study. On the other hand, this is the first report on the a_w, deliquescence, and water absorption of ABS/MA mixtures. The eutonic composition for AS/MA mixtures was found to be 66.8 MA dry wt % (MA dry wt % = MA mass × 100/(AS mass + MA mass) with a DRH of 0.437. The eutonic composition for the ABS/MA mixtures was lower than for the AS/MA mixtures: 20.9 MA dry wt % with a DRH of 0.327. Measured a_w of liquid AS/MA and ABS/MA solutions is compared with an extended Zdanovskii−Stokes−Robinson expression, obtaining a good agreement (error < 5−6%). The expression was used to predict water uptake of mixtures and might be useful to interpret particle hygroscopic growth experiments. Comparison of the AS/MA and ABS/MA systems indicates that ABS reduces the DRH and enhances water uptake, relative to mixtures with AS. The results confirm that ambient particles containing sulfate and water-soluble organic compounds can remain liquid or partially liquid at very low ambient RH conditions, especially if the sulfate is not completely neutralized.

1. Introduction

Atmospheric aerosols are ubiquitous and play an important role in atmospheric processes such as radiative transfer, heterogeneous reactions, and chemical and physical uptake of gases. Also, they have significant impacts on climate, visibility, and human health.[1,2] The specific effect of the aerosol on these processes depends on its size, chemical composition, and phase.[3,4] Aerosols generally contain mixtures of sulfates, nitrates, ammonium, organic material, sea salt, and other inorganic species, hydrogen ions, and water. In the inorganic fraction of the aerosol, sulfate and ammonium are usually the predominant ions in the fine particles.[5] Depending on the availability of ambient ammonia, sulfate might be partially or totally neutralized.[6,7] The organic fraction of the ambient aerosol is a complex mixture of thousands of different compounds,[8] which can be water soluble or insoluble. Among the soluble compounds, dicarboxylic acids, including malonic acid (MA), were identified in many sites.[9,10]

The phase of the aerosol is determined by its composition, temperature, and ambient relative humidity (RH). Phase diagrams as a function of RH and temperature for inorganic compounds, such as ammonium nitrate and sulfate, sodium chloride, and other salts found in ambient aerosols, have been widely studied.[11,12] However, the effect of organic compounds on the phase transitions of inorganic aqueous mixtures is actively being studied by many groups.[3,13]

Mixtures of ammonium sulfate (AS) and MA (as well as other soluble organic compounds) have previously been chosen as models for ambient aerosols, and several studies on the RH-dependent phase transitions (deliquescence and efflorescence) and hygroscopic growth of these mixtures were published.[14−21] Choi and Chan[14] studied the effect of some organic compounds (including MA) on the water cycles, crystallization, and deliquescence relative humidity (DRH) of sodium chloride and AS using an electrodynamic balance (EDB). Brooks et al.[15] and Wise et al.[16] reported solubility, DRH, and eutonic composition of pure dicarboxylic acids and AS/dicarboxylic acids (including MA) bulk mixtures. Wise et al. also reported water activity (a_w) of some aqueous solutions of AS/dicarboxylic acids mixtures. Parsons et al.[17] reported total deliquescence and crystallization RH of AS particles internally mixed with water soluble organics (including MA) with an organic mass fraction of less than 0.6 using an optical microscope coupled to a flow cell. Braban et al.[18] studied the phase transitions of the system AS/MA as a function of RH using infrared extinction spectroscopy. The hygroscopic behavior of internally mixed particles of AS and dicarboxylic acids (including MA) using tandem differential mobility analyzers (TDMA) was studied by Hämeri et al.[19] and Prenni et al.[20] All of these reports concluded that the presence of MA lowers the DRH and reduces the hygroscopic growth of

* Corresponding author. E-mail: dara@ciq.uaem.mx.

10.1021/jp063850v CCC: $33.50
Published on Web 10/17/2006

AS. Finally, Marcolli et al.[21] measured a_w of saturated aqueous solutions of mixtures of several dicarboxylic acids (including MA) and ammonium nitrate and sulfate, and sodium chloride. They found that a mixture of five dicarboxylic acids reduces the DRH relative to the pure acids; a further reduction in DRH is obtained when an inorganic salt is added.

There is only one study on the RH-dependent phase transitions of mixtures of ammonium bisulfate (ABS) and MA: Parsons et al.[22] reported crystallization RH of aqueous inorganic/MA particles with AS, letovicite, and ABS. Furthermore, to the best of our knowledge, there are no reports on the deliquescence RH of ABS/MA mixtures or a_w of their aqueous solutions.

In this work, measurements of a_w of aqueous solutions of AS/MA and ABS/MA over the full range of composition at 25 °C are presented. The composition and a_w of saturated aqueous solutions with respect to at least one of the solutes also were measured. The resulting data were used to plot equilibrium phase diagrams, which include a_w, DRH, eutonic composition, eutonic DRH, and equilibrium phases as a function of total and dry composition. This work complements previous reports on the thermodynamic properties of the AS/MA system as it covers composition ranges that were not previously investigated in a single study and summarizes the data in phase diagrams that facilitate its interpretation. Furthermore, DRH of ABS/MA mixtures and a_w of their aqueous solutions are reported for the first time. The data measured were used to calculate water uptake of AS/MA and ABS/MA mixtures. Finally, the effect of sulfate acidity on the thermodynamic properties of mixtures with MA is discussed.

2. Experimental Procedures

An Aqualab 3TE (Decagon Devices, Nelson Court, WA) was used to determine a_w of aqueous mixtures of MA ($HOOC-CH_2-CH_2-COOH$) with AS ($(NH_4)_2SO_4$) or ABS (NH_4HSO_4). The Aqualab 3TE determines a_w of the samples by measuring the dew point temperature of the water vapor in equilibrium with the sample. The instrument consists of a sealed chamber where the sample is equilibrated with the headspace. The dew point temperature is detected with a controlled-temperature mirror and a beam of light directed onto the mirror and reflected into a photodetector cell that senses the change in reflectance when condensation occurs on the mirror. The precision of the Aqualab 3TE is ±0.003 activity units. The a_w of the solution corresponds to the equilibrium RH if the vapor phase is considered to behave as an ideal gas; consequently a_w and RH are used interchangeably in this paper.

Bulk mixtures of MA (Sigma−Aldrich, 99%) with AS (Fluka, ≥99.5%) or ABS (Aldrich, 99.99%) in deionized water (18 μΩ·cm) were prepared gravimetrically. Mixtures were stirred until the entire solid was dissolved. In some cases, complete dissolution was achieved only after stirring overnight, particularly when the concentration of the mixture was close to the solubility limit. Uncertainties on the concentration of the mixtures were calculated from the precision of the balance (±0.01 g) and the measured mass of each component and are estimated to be between 0.3 and 3.5 wt %.

A series of aqueous AS/MA and ABS/MA mixtures were prepared keeping the concentration of one of the solutes constant, while the concentration of the other solute was progressively increased (the water concentration was reduced proportionally) until some solid remained undissolved even after overnight stirring. Saturation, or the solubility limit, was established as the concentration of the last completely liquid mixture in the series. The a_w for all solutions was measured using the Aqualab 3TE at 25 ± 0.2 °C. Overnight stirring was used as the upper limit for the stirring time, because solutions that were not completely dissolved did not show changes in their activity after further stirring.

The a_w of aqueous solutions of pure AS, ABS, and MA, and AS/MA and ABS/MA aqueous mixtures were calculated with commonly used thermodynamic models. The AIM III[23] was used to calculate a_w of aqueous AS and ABS solutions. The a_w of aqueous MA solutions were calculated with the UNIFAC model,[24] using the group interaction parameter for CH_2 from Hansen et al.;[25] for H_2O and COOH, the revised group interaction parameters reported by Peng et al.[26] were used. The a_w of AS/MA and ABS/MA aqueous mixtures was computed using the Zdanovskii−Stokes−Robinson (ZSR) equation in its original[27] and extended versions:[28]

$$\frac{1}{m} = \frac{x_a}{m_a^0} + \frac{x_b}{m_b^0} + x_a x_b (A + B a_w) \qquad (1)$$

where m is the total molality of solutes a and b in the mixture; x_a and x_b are the mole fractions of a and b in the mixture; m_a^0 and m_b^0 are the molalities of aqueous solutions of pure a and b at the same a_w as the mixture; and A and B are parameters whose values are determined by fitting all the experimental a_w data. Equation 1 represents the extended version of the ZSR equation; the original ZSR expression is obtained with A and B equal to zero. The extended ZSR model has been recently applied to aqueous solutions containing inorganic electrolytes and dicarboxylic acids.[29]

3. Results and Discussion

3.1. AS and MA. Figure 1 shows the a_w measured for liquid water/AS/MA (W/AS/MA) mixtures. Concentration is expressed in total weight percent of one component in the ternary mixture (for example, MA wt % = MA mass × 100/(W mass + AS mass + MA mass)). Figure 1 also shows the calculated a_w using the AIM III model, UNIFAC, and the extended ZSR model (with $A = -0.02$ and $B = -0.05$), as described in the previous section. The percent error of the original (with $A = B = 0$) and the extended ZSR models relative to the measured a_w is shown in Figure 2 as a function of water concentration. Figure 2 shows that the original ZSR model provides a good approximation for relatively dilute solutions (water wt % > ∼36) with errors below 5%. However, as the water content decreases, the model becomes less accurate. On the other hand, the correction to the ZSR equation causes an improvement in accuracy with errors below 5% for even the most concentrated solutions.

The RH over a saturated aqueous solution corresponds to the RH at which the dry AS/MA mixture will fully deliquesce (deliquescence relative humidity, DRH). Figure 3 shows the DRH as a function of MA dry weight percent (MA d-wt % = MA mass × 100/(AS mass + MA mass)). The DRH of the mixtures is lower than the DRH of the pure solids. The lowest DRH corresponds to the eutonic deliquescence relative humidity (EDRH).

Table 1 summarizes the DRH and solubility results for the pure solutes and the eutonic mixture. For comparison purposes, previous measurements[14−18,20,21,26,30−35] of DRH and solubility for pure AS and MA, as well as for AS/MA mixtures, are also shown in Figure 3 and Table 1. The data obtained in this work is in good agreement (within experimental error) with other DRH and solubility measurements for pure AS and MA, and for AS/MA mixtures with MA d-wt % < 57. However, there

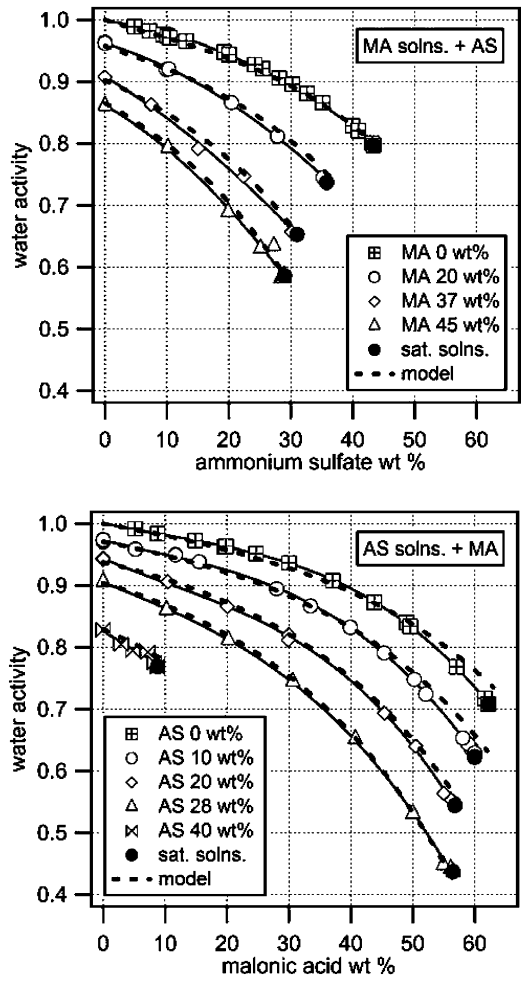

Figure 1. The a_w at 25 °C for aqueous AS/MA solutions as a function of weight percent of one of the solutes (the concentration of the other remains constant in each series). Black circles correspond to saturated solutions. Uncertainty bars are smaller than the size of the symbols. Solid lines are polynomial fits to data. Dotted lines were calculated using AIM III and UNIFAC for the binary solutions and the extended ZSR expression ($A = -0.02$ and $B = -0.05$) for the ternary ones.

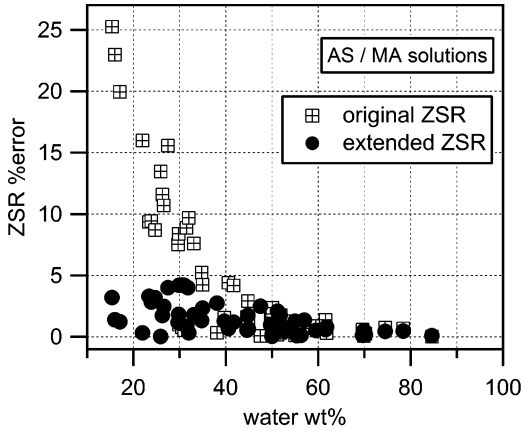

Figure 2. The a_w percent error of the original and extended ZSR expressions as a function of water weight percent for the system AS/MA.

are discrepancies between this work and the DRH reported by Brooks et al.[15] for mixtures with MA d-wt % > 57. The eutonic composition reported by these authors does not agree with this work either. Brooks et al. used bulk samples for their measurements, and the method for preparing the solutions was similar to ours. A possible reason for the disagreement between the

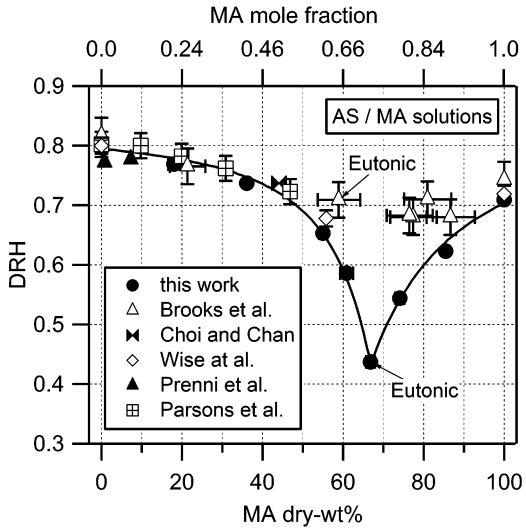

Figure 3. DRH at 25 °C as a function of MA dry wt % for AS/MA mixtures. The solid line is a polynomial fit to data from this study. Top axis is in MA dry mole fraction [mole MA/(mole AS + mole MA)]. Previously measured values of DRH are shown: Brooks et al.[15] (24 °C); Choi and Chan[14] (20−23 °C); Wise et al.[16] (25 °C); Prenni et al.[20] (30 °C); and Parsons et al.[17] (20 °C). Eutonic points as reported in this work and by Brooks et al. are marked in the figure.

reported eutonic compositions is the stirring time used for complete dissolution. Brooks et al. do not mention the stirring time they used. However, for this study, solutions with concentrations close to saturation needed several hours and, sometimes, overnight stirring before complete dissolution. Insufficient stirring might result in reporting a lower eutonic composition, as Brooks et al. do. The source of the discrepancies between RH measurements is not known.

All the information in Figures 1 and 3 was summarized in one single ternary diagram, shown in Figure 4. The diagram includes DRH, eutonic composition, EDRH, phase equilibrium lines, and equilibrium RH over liquid solutions as a function of total mixture composition. Lines of constant RH were calculated using the extended ZSR model so that equilibrium RH over liquid solutions can be read directly from the diagram. (Saturated solution + solid) − (eutonic solution + solid) equilibrium lines and solid equilibrium lines (lines from the bottom apex of the triangle to the eutonic composition) were drawn taking into account that the eutonic solution is the most concentrated solution with respect to both solutes and assuming that the solids in equilibrium with the saturated solutions are AS and MA (see below for evidence). The ternary diagram shows that W/AS/MA ternary mixtures always will be liquid for RH larger than the DRH of AS. For RH between the DRH of pure AS and the EDRH, mixtures can be liquid or a saturated solution in equilibrium with a solid. Conditions of RH below the EDRH are not represented in the diagram because, under those conditions, only solid binary AS/MA mixtures are expected.

Note that there are some discrepancies between the measured DRH (shown in Figure 1) and the calculated DRH (shown in Figure 4) especially on the MA branch (to the right of the eutonic composition). For example, the measured DRH for a pure MA solution is 0.709, while the DRH shown in Figure 4 for the same solution is close to 0.75. The source of this discrepancy is the error of the UNIFAC model for concentrations close to MA saturation. Figure 1 shows that UNIFAC predicts that a_w of a pure MA saturated solution is 0.745 instead of 0.709, as it was measured. This error propagates to a_w calculations using ZSR for aqueous AS/MA mixtures with relatively high

TABLE 1: Summary of Results at 25 °C[a]

	solubility in water (wt %)	DRH	MA dry wt %
AS	43.4 ± 1.2	0.797	
	(43.3,[b] 43.4,[c] 43.2[d])	(0.80,[b] 0.817,[c] 0.802,[d] 0.79,[e] 0.80,[f] 0.79,[g] 0.793,[h] 0.81[i])	
ABS	77.2 ± 1.7	0.402	
	(76[b])	(0.40,[b] 0.39[e])	
MA	62.2 ± 1.5	0.709	
	(62.2,[c] 61.3[d])	(0.743[c], 0.724[d], 0.652,[j] 0.69,[k] 0.72[l])	
AS/MA eutonic	84.5 ± 2.0[j]	0.437	66.8 ± 1.1
	(69.2[c])	(0.709[c])	(58.9[c])
ABS/MA eutonic	82.1 ± 1.4[j]	0.327	20.9 ± 0.3

[a] Uncertainty of DRH is ± 0.003. Other reported values are given in parentheses. [b] 25 °C (Tang and Munkelwitz, 1994).[30] [c] 24 °C (Brooks et al., 2002).[15] [d] 25 °C (Marcolli et al., 2004).[21] [e] Room temperature (Cziczo et al., 1997).[31] [f] 22 °C (Onasch et al., 1999).[32] [g] 22−26 °C (Cruz and Pandis, 2000).[33] [h] 30 °C (Prenni et al., 2003).[20] [i] 20 °C (Braban and Abbat, 2004).[18] [j] 25 °C (Peng et al., 2001).[26] [k] 20.8 °C (Braban et al., 2003.[34] [l] 25 °C (Parsons et al., 2004).[35] [m] Solubility is given in solute wt % = (inorganic mass + MA mass) × 100/(W mass + inorganic mass + MA mass).

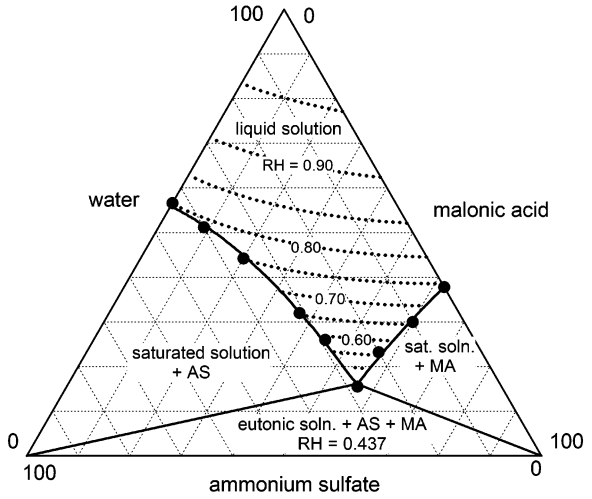

Figure 4. Triangular equilibrium phase diagram for W/AS/MA mixtures at 25 °C. Circles are the saturated solutions from Figure 1. Solid lines represent phase equilibrium lines. Dotted lines represent constant RH conditions and were calculated using eq 1.

amounts of MA. The above discussion indicates that the accuracy of the ZSR equation is limited by the accuracy of UNIFAC.

It has been suggested that upon crystallization, solutions containing AS and MA can form other salts such as ABS, letovicite, and ammonium hydrogen malonate but at very low concentrations.[18] To test the identity of the solid in equilibrium with saturated solutions, we measured the a_w of some ternary mixtures in which some undissolved solid was still present after several hours of stirring. Figure 5A shows a ternary diagram with lines that represent 10 AS wt % and 20 MA wt % mixtures. The upper section of each line (from the top apex of the triangle to the saturated solution−solid equilibrium line) represents mixtures that are completely liquid. In contrast, the portion of the line below the equilibrium line represents partially liquid mixtures. Figure 5A also shows the total concentration of mixtures with 10 AS wt % or 20 MA wt %, which remained as saturated solutions in equilibrium with a solid phase after several hours of stirring. The composition of the saturated liquid solution was determined by drawing a line from the apex of the triangle to the point corresponding to each mixture and by extending the line until it crosses the saturated-solution−solid-equilibrium line, as shown in Figure 5A. Assuming that the solution is saturated only with either AS or MA, the identity and the amount of the solid remaining in the mixture can be calculated from the difference in composition between the mixture and the saturated solution. The remaining solid was MA in the 10 wt % AS mixtures, whereas the solid was AS in the 20 wt % AS mixtures. Figure 5B shows the measured and expected a_w of the latter mixtures. The expected a_w was obtained with the extended ZSR model. The good agreement between measured and expected values of a_w suggests that AS and MA are the main solids in equilibrium with the aqueous saturated solutions, and that the concentration of any other solid present is negligible. Furthermore, this discussion also suggests that a mixture less concentrated in AS than the eutonic mixture will be in equilibrium with solid MA. In contrast, mixtures more concentrated in AS than the eutonic mixture will be in equilibrium with solid AS. It is important to note that these arguments are based upon results obtained under equilibrium conditions, and that crystallization often occurs under metastable conditions. Hence, other solid phases might form upon efflorescence of aqueous mixtures.

The data presented above can be used to calculate water absorption of AS/MA mixtures. For example, Figure 6A presents the expected solute wt % [(AS mass + MA mass)/(W mass + AS mass + MA mass)] as a function of RH for four AS/MA mixtures: the eutonic mixture (66.8 MA d-wt %), and 10, 50, and 90 MA d-wt %. For reference, Figure 6B shows the same mixtures in a ternary diagram. To calculate the water absorption lines similarly as in Figure 5B, we calculated the equilibrium RH over mixtures with constant MA d-wt % and an increasing amount of water. Figure 6 shows that for compositions below the EDRH, all the mixtures are expected to be solid (solute wt % = 100) and not to uptake water when RH is increased. As RH increases further, there is a discontinuity at the EDRH because deliquescence (partial or total) of the solid mixtures occurs. The eutonic mixture acts like a pure solid and completely deliquesces at the EDRH. In contrast, noneutonic mixtures deliquesce only partially at the EDRH, and they continue gradually deliquescing until the total DRH is reached (marked as DRH in Figure 6A) and they become completely liquid. At this RH, a second discontinuity in solute wt % is observed, which is less pronounced for mixture compositions close to the eutonic composition (note that the eutonic mixture only shows the first discontinuity). The water absorption behavior presented in Figure 6A can be useful to interpret particle hygroscopic growth experiments. For example, Prenni et al.[20] did not observed a distinct deliquescence during hygroscopic growth experiments of 50 MA d-wt % particles using a humidified tandem differential mobility analyzer (HTDMA) at 30 °C. They explained this observation by suggesting that the particles were not crystallized at the beginning of the experiment and remained liquid as the RH was increased from <0.05 to >0.9. However, Figure 6 suggests that the results of Prenni et al.[20] also can be

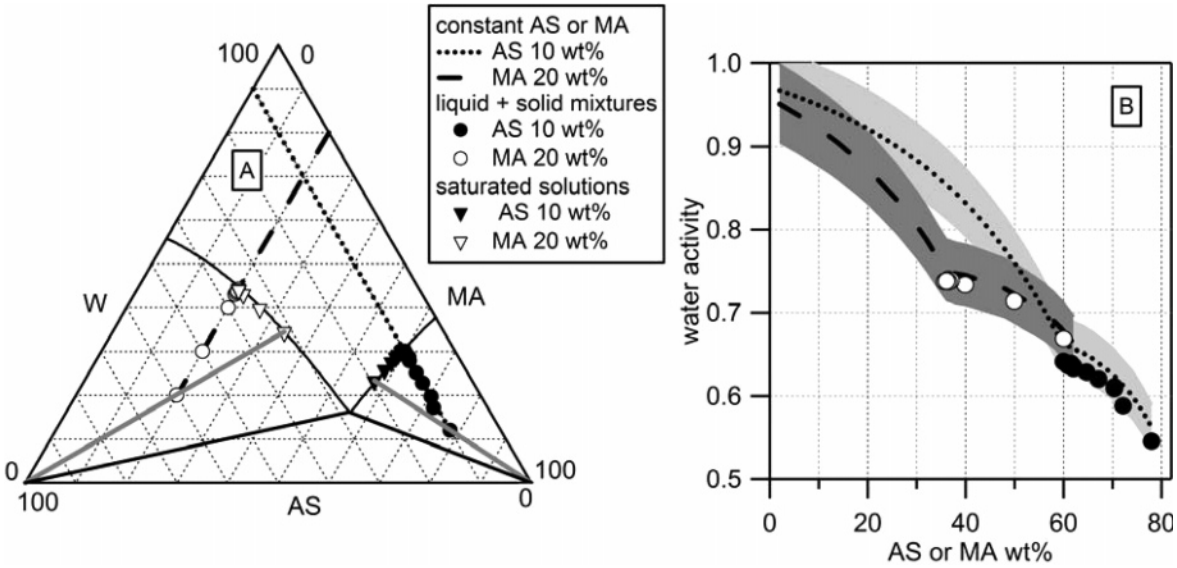

Figure 5. Panel A: triangular equilibrium phase diagram for W/AS/MA mixtures. Dotted and dashed lines are lines of constant weight percent of one of the solutes. Circles represent the total composition of partially liquid mixtures. Triangles represent the composition of the saturated solution in equilibrium with a solid. Grey lines show how to determine the composition of the saturated solutions. Panel B: a_w for W/AS/MA mixtures as a function of weight percent of one of the solutes. Circles represent the measured a_w of the mixtures. Dotted and dashed lines represent the calculated a_w using the extended ZSR model. Shaded areas represent the ± 5% error of the model.

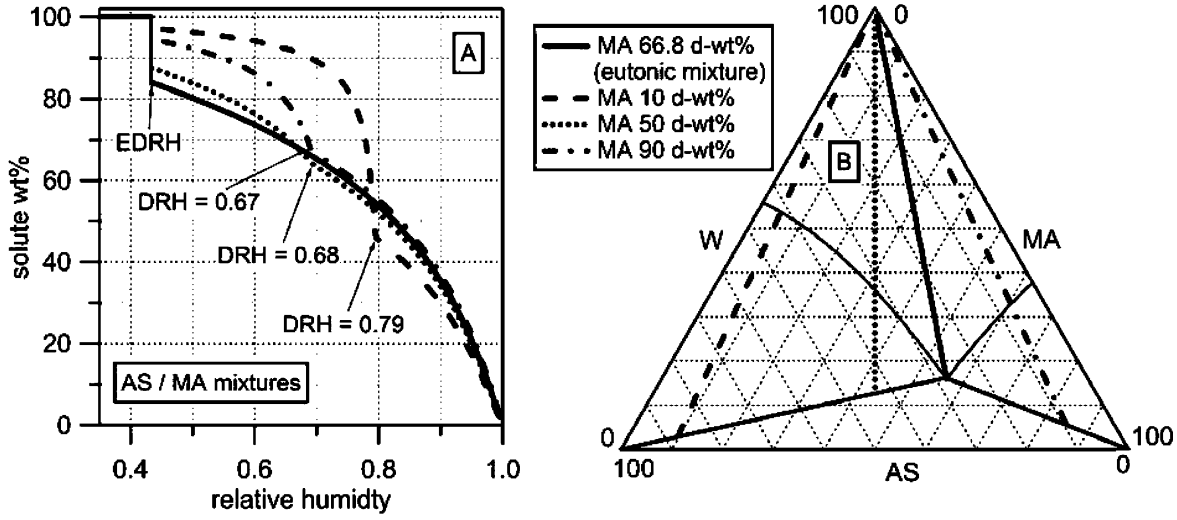

Figure 6. Panel A: solute weight percent [(AS mass + MA mass)/(AS mass + MA mass + W mass)] as a function of RH for AS/MA mixtures with constant MA d-wt %. Panel B: triangular equilibrium phase diagram showing the total concentration of the same mixtures as panel A.

explained by a scenario where particles were solid at the beginning of the experiment and gradually deliquesced when RH was increased. In this case, the subtle discontinuous change in hygroscopic growth when particles completely deliquesced might have been difficult to detect, because of the uncertainty of their experiment.

Figure 7 compares curves of water uptake vs RH calculated using the extended ZSR equation with data previously reported by Choi and Chan[14] and Wise et al.[16] Both groups measured a_w of bulk samples of AS/MA mixtures; Choi and Chan also measured the hygroscopic growth properties of (AS/MA particles using a scanning electrodynamic balance (SEDB). Figure 7 shows that bulk measurements agree with the extended ZSR calculation. On the other hand, the SEDB growth measurements agree relatively well with the ZSR above the DRH (when particles are liquid), but there is a considerable difference at lower RH (when particles are expected to be solid or partially solid). A possible reason for the discrepancy at low RH is the density of the particles, which is needed to calculate the solute wt % from the SEDB experiments and which is estimated using a simple volume additivity rule.[14]

3.2. ABS and MA. The a_w of ABS/MA mixtures also were determined for the full range of compositions, and the results are shown in Figure 8. Mixtures with 67 ABS wt % also were studied, but the results are omitted in the figure for clarity. The a_w of solutions calculated with the AIM III model and the ZRS model (eq 1 with $A = B = 0$) are in good agreement with experimental data. Figure 9 shows that for the ABS/MA system, the ZSR equation provides a good approximation (errors <6%) in the whole range of composition without any correction. As it was discussed before, the accuracy of the ZSR equation is limited by the accuracy of the UNIFAC model.

Solubility and DRH results for pure ABS and ABS/MA mixtures are summarized in Table 1. Previous measurements for pure ABS[30,31] also are included in the table and are in good agreement (within experimental uncertainties) with our results.

Figure 10 shows the ternary phase diagram for the system W/ABS/MA, which presents the same information as Figure 4

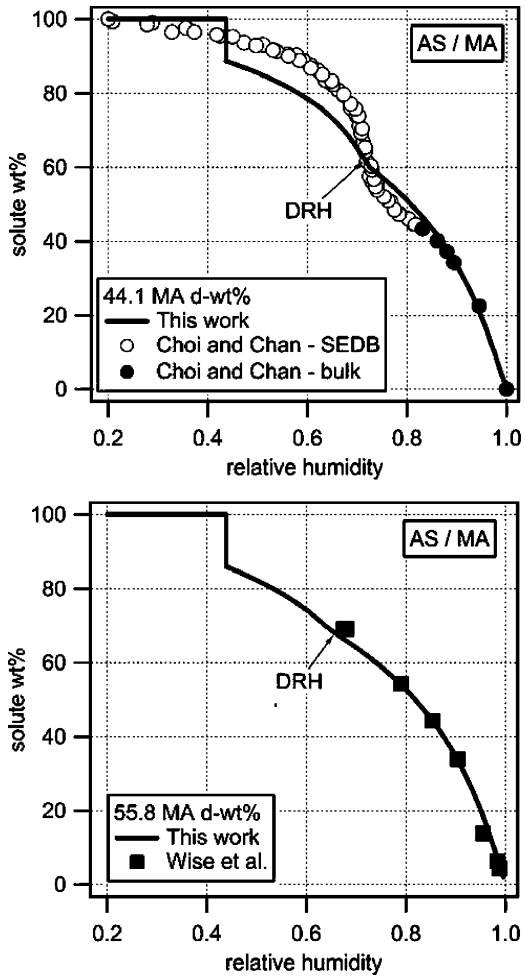

Figure 7. Solute weight percent as a function of RH for AS/MA mixtures with constant MA d-wt %, calculated using the extended ZSR model and measured by Choi and Chan[14] (20−23 °C) and Wise et al.[16] (25 °C).

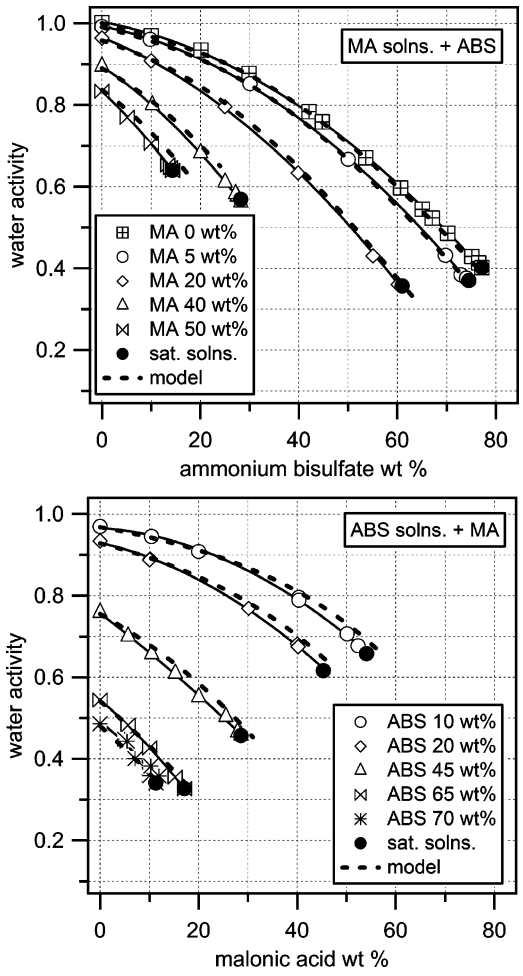

Figure 8. The a_w at 25 °C for aqueous ABS/MA solutions as a function of weight percent of one of the solutes (the concentration of the other remains constant in each series). Black circles correspond to saturated solutions. Error bars are smaller than the size of the symbols. Solid lines are polynomial fits to data. Dotted lines were calculated using the AIM III model for the binary solutions and the original ZSR expression for the ternary ones.

for the W/AS/MA system. To determine the identity of the solids in equilibrium with the saturated solutions, Figure 11 shows the measured a_w for ABS/MA mixtures with 5 and 40 MA wt %, which remained partially liquid after several hours of stirring. The figure also presents the expected a_w for the same mixtures assuming that the solids in equilibrium with the liquid solutions below the DRH are ABS and MA for the 5 and 40 MA wt % mixtures, respectively. The good agreement between measured and expected a_w suggests that, if other solids are in equilibrium with the mixtures, their concentration is negligible.

DRH as a function of MA d-wt % for ABS/MA and AS/MA mixtures are shown in Figure 12. For MA d-wt % < ∼60, the DRH is lower for mixtures with ABS than AS/MA mixtures. This implies that ABS/MA mixtures can remain liquid or partially liquid to lower RH than AS/MA mixtures.

Water uptake curves for ABS/MA and AS/MA mixtures are shown in Figure 13. To determine the effect of sulfate being totally or partially neutralized, the figure compares mixtures with the same MA to sulfate (SO_4^{2-}) ratio (MA/S = MA mass/sulfate mass). The start of deliquescence (at the EDRH) and the total DRH are lower for the ABS/MA mixtures relative to the equivalent AS/MA mixtures, restating the fact that ABS/MA mixtures can remain liquid or partially liquid to lower RH than AS/MA mixtures. Figure 13 also shows that ABS/MA mixtures absorb more water than the equivalent AS/MA mixtures, implying that the fact that the sulfate is not completely neutralized enhances water uptake.

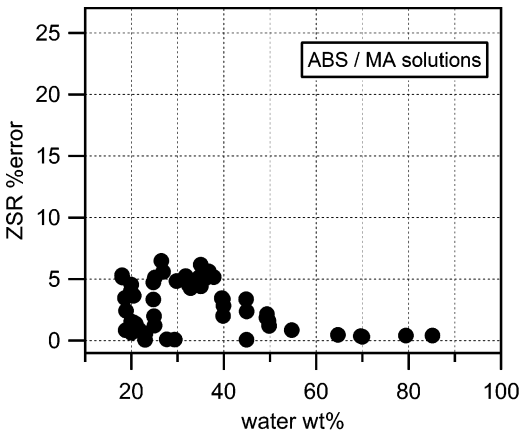

Figure 9. The a_w percent error of the ZSR expression as a function of water weight percent for the system ABS/MA.

4. Conclusions and Atmospheric Implications

In this paper, we measured solubility in water, a_w, DRH, eutonic composition, and EDRH of AS/MA and ABS/MA mixtures over the full range of compositions at 25 °C. The information was used to plot phase diagrams that present the equilibrium phase of the mixtures as a function of total composition, dry mixture composition, water content, and

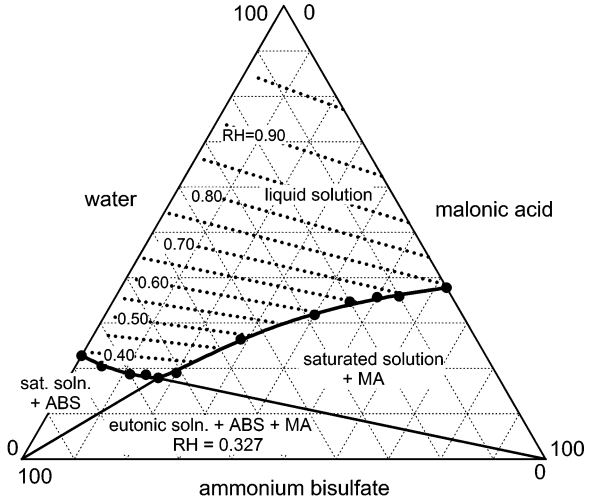

Figure 10. Triangular equilibrium phase diagram for W/ABS/MA mixtures at 25 °C. Circles are the saturated solutions from Figure 8. Solid lines represent phase equilibrium lines. Dotted lines represent constant RH conditions and were calculated using the ZSR model.

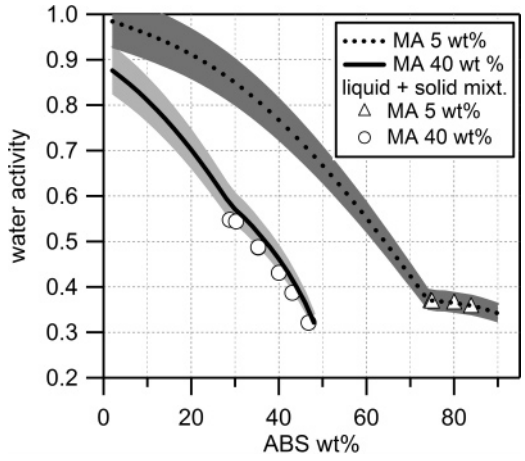

Figure 11. The a_w for aqueous W/AS/MA solutions as a function of weight percent of one of the solutes. Circles represent the measured a_w of partially liquid mixtures. Dotted and dashed lines represent the calculated a_w using the ZSR model. Shaded areas represent the ± 6% error of the model.

ambient RH. The thermodynamic data obtained might be useful to develop and test thermodynamic models of atmospheric aerosols[36] and, especially, data for the ABS/MA mixtures, which has not been reported before. Furthermore, the presentation of all the data in one single ternary phase diagram simplifies its interpretation and can be used to predict water uptake of aerosols and to interpret hygroscopic growth experiments.

The commonly used ZSR model was compared with experimental a_w for the AS/MA and ABS/MA systems. The error of the model depends on the water content of the mixture, and it is a good approximation (error < 5%) only for the more dilute solutions of AS/MA (water concentration larger than ~36 wt %). For more concentrated solutions, it is necessary to use a correction to the model to obtain more accurate values. On the other hand, for the AMS/MA solution, the ZSR model has errors lower the 5% in the complete range of concentrations without any correction. The accuracy of the ZSR model is limited by the accuracy of the models used to calculate the a_w of the binary solutions.

The effect of MA on the DRH of AS is larger than had been determined before, especially for compositions close to the eutonic composition. Accordingly, MA also has a large effect

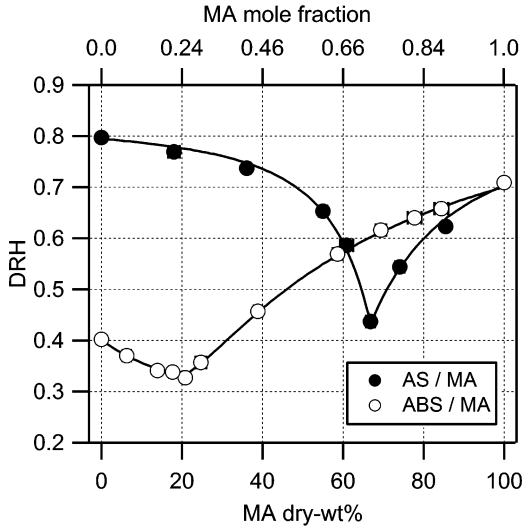

Figure 12. DRH at 25 °C as a function of MA dry wt % for AS/MA and ABS/MA mixture. Solid lines are polynomial fits to data. Error bars are smaller than the size of the symbols. Top axis is in MA dry mole fraction: mole MA/(mole MA + mole inorganic).

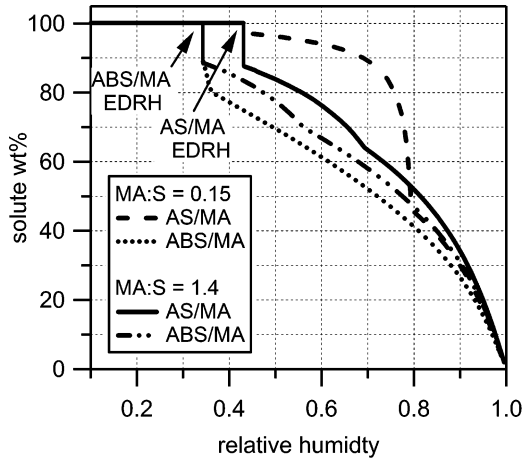

Figure 13. Solute weight percent [(inorganic mass + MA mass)/(W mass + inorganic mass + MA mass)] as a function of RH for ABS/MA and AS/MA mixtures with equal MA to sulfate ration (MA/S = MA mass/sulfate mass). MA/S = 0.15 mixtures, correspond to 10 and 11.3 MA d-wt % for AS/MA and ABS/MA mixtures, respectively. MA/S = 1.4 mixtures, correspond to 50 and 53.4 MA d-wt % for AS/MA and ABS/MA mixtures, respectively.

on the DRH of ABS. The results indicate that ABS reduces the DRH and enhances water uptake, relative to mixtures with AS, for mixtures with MA dry wt % < 60. Ambient particles containing non-neutralized sulfate have been observed in several sites;[6,7] hence, the effect of acidity on thermodynamic properties of the aerosol might have important atmospheric implications.

Ambient aerosols are mixtures much more complex than the ones studied here in which the organic fraction contains a large amount of different soluble and insoluble species. Marcolli et al.[21] showed that the DRH of mixtures of inorganic salts with dicarboxylic acids vary inversely to the number of organic components in the solution and suggested that tropospheric aerosols will remain liquid or partially liquid at very low RH. This work confirms this conclusion by showing that ternary mixtures have a very low DRH. The presence of more organic compounds in ambient particles than in the mixtures studied here would further reduce the DRH. This effect might be even more pronounced if the sulfate is not completely neutralized.

Acknowledgment. This research was funded by Consejo Nacional de Ciencia y Tecnología (CONACyT), México.

Supporting Information Available: Tables with all the experimental data are presented for the AS/MA/W and ABS/MA/W systems (Tables S1 and S2). This material is available free of charge via the Internet at http://pubs.acs.org.

References and Notes

(1) IPCC. "IPCC Third Assessment Report: Climate Change 2001"; Intergovernmental Panel of Climate Change, 2001.

(2) McMurry, P.; Sheperd, M.; Vickery, J. *Particulate Matter Science for Policy Makers. A NARSTO Assessment*; Cambridge University Press: New York, 2004.

(3) Pöschl, U. *Angew. Chem., Int. Ed.* **2005**, *44*, 7520.

(4) Satheesha, S. K.; Moorthy, K. K. *Atmos. Environ.* **2005**, *39*, 2089.

(5) Seinfeld, J. H.; Pandis, S. N. *Atmospheric Chemistry and Physics. From Air Pollution to Climate Change*; John Wiley and Sons: New York, 1998.

(6) Pathaka, R. K.; Louie, P. K. K.; Chan, C. K. *Atmos. Environ.* **2004**, *38*, 2965−2974.

(7) Salcedo, D.; Onasch, T. B.; Dzepina, K.; Canagaratna, M. R.; Zhang, Q.; Huffman, J. A.; DeCarlo, P. F.; Jayne, J. T.; Mortimer, P.; Worsnop, D. R.; Kolb, C. E.; Johnson, K. S.; Zuberi, B.; Marr, L. C.; Volkamer, R.; Molina, L. T.; Molina, M. J.; Cardenas, B.; Bernabé, R. M.; Márquez, C.; Gaffney, J. S.; Marley, N. A.; Laskin, A.; Shutthanandan, V.; Xie, Y.; Brune, W.; Lesher, R.; Shirley, T.; Jimenez, J. L. *Atmos. Chem. Phys.* **2006**, *6*, 925−946.

(8) Mader, B. T.; Yu, J. Z.; Xu, J. H.; Li, Q. F.; Wu, W. S.; Flagan, R. C.; Seinfeld, J. H. *J. Geophys. Res.* **2004**, *109*, 6206.

(9) Yu, L. E.; Shulman, M. L.; Kopperud, R.; Hildemann, L. M. *Environ. Sci. Technol.* **2005**, *39*, 707.

(10) Wang, H. B.; Kawamura, K.; Yamazaki, K. *J. Atmos. Chem.* **2006**, *53*, 43.

(11) Wexler, A. S.; Clegg, S. L. *J. Geophys. Res.* **2002**, *107*, D14.

(12) Seinfeld, J. H. *AIChE J.* **2004**, *50*, 1096.

(13) Kanakidou, M.; Seinfeld, J. H.; Pandis, S. N.; Barnes, I.; Dentener, F. J.; Facchini, M. C.; Dingenen, R. V.; Ervens, B.; Nenes, A.; Nielsen, C. J.; Swietlicki, E.; Putaud, J. P.; Balkanski, Y.; Fuzzi, S.; Horth, J.; Moortgat, G. K.; Winterhalter, R.; Myhre, C. E. L.; Tsigaridis, K.; Vignati, E.; Stephanou, E. G.; Wilson, J. *Atmos. Chem. Phys.* **2005**, *5*, 1053.

(14) Choi, M. Y.; Chan, C. K. *Environ. Sci. Technol.* **2002**, *36*, 2422.

(15) Brooks, S. D.; Wise, M. E.; Cushing, M.; Tolbert, M. A. *Geophys. Res. Lett.* **2002**, *29*, art. no. 1917.

(16) Wise, M. E.; Surratt, J. D.; Tolbert, M. A. *J. Geophys. Res.* **2003**, *108*, 4638.

(17) Parsons, M. T.; Knopf, D. A.; Bertram, A. K. *J. Phys. Chem. A* **2004**, *108*, 11600.

(18) Braban, C. F.; Abbatt, J. P. D. *Atmos. Chem. Phys.* **2004**, *4*, 1451.

(19) Hämeri, K.; Charlson, R.; Hansson, H.-C. *AIChE J.* **2002**, *48*, 1309.

(20) Prenni, A. J.; DeMott, P. J.; Kreidenweis, S. M. *Atmos. Environ.* **2003**, *37*, 4243.

(21) Marcolli, C.; Luo, B.; Peter, T. *J. Phys. Chem. A* **2004**, *108*, 2216.

(22) Parsons, M. T.; Riffell, J. L.; Bertram, A. K. *J. Phys. Chem. A* **2006**, *110*, 8108.

(23) Clegg, S. L.; Brimblecombe, P.; Wexler, A. S. *J. Phys. Chem. A* **1998**, *102*, 2155.

(24) Fredenslund, A.; Jones, R. L.; Prausnitz, J. M. *AIChE J.* **1975**, *21*, 1086.

(25) Hansen, H. K.; Rasmussen, P.; Fredenslund, A.; Schiller, M.; Gmehling, J. *Ind. Eng. Chem. Res.* **1991**, *30*, 2352.

(26) Peng, C.; Chan, M. N.; Chan, C. K. *Environ. Sci. Technol.* **2001**, *35*, 4495.

(27) Stokes, R. H.; Robinson, R. A. *J. Phys. Chem.* **1966**, *70*, 2126.

(28) Clegg, S. L.; Seinfeld, J. H.; Edney, E. O. *Aerosol Sci.* **2003**, *34*, 667−690.

(29) Clegg, S. L.; Seinfeld, J. H. *J. Phys. Chem. A* **2006**, *110*, 5692.

(30) Tang, I. N.; Munkelwitz, H. R. *J. Geophys. Res.* **1994**, *99*, 18.

(31) Cziczo, D. J.; Nowak, J. B.; Hu, J. H.; Abbatt, J. P. D. *J. Geophys. Res.* **1997**, *102*, 18843.

(32) Onasch, T. B.; Siefert, R. L.; Brooks, S. D.; Prenni, A. J.; Murray, B.; Wilson, M. A.; Tolbert, M. A. *J. Geophys. Res.* **1999**, *104*, 21.

(33) Cruz, C. N.; Pandis, S. N. *Environ. Sci. Technol.* **2000**, *34*, 4313.

(34) Braban, C. F.; Carroll, M. F.; Styler, S. A.; Abbatt, J. P. D. *J. Phys. Chem. A* **2003**, *107*, 6594.

(35) Parsons, M. T.; Mak, J.; Lipetz, S. R.; Bertram, A. K. *J. Geophys. Res.* **2004**, *109*.

(36) Raatikainen, T.; Laaksonen, A. *Atmos. Chem. Phys.* **2005**, *5*, 2475−2495.